ISSN 1392-1207. MECHANIKA. Vol. 30, No. 3, 2024: 236–243

Impact Analysis of Key Engine Parameters on Piston Lubrication and Friction Performance in Diesel Engines Using GT-SUITE Program

Brahim MENACER*, Abdelkader SOUALMIA, Sunny NARAYAN***, Moaz AL-LEHAIBI******

**Laboratoire des systèmes complexe (LSC), Ecole Supérieure en Génie Electrique et Energétique ESGEE Oran, Chemin Vicinal N9, Oran 31000, Algeria,*
E-mails: acer.msn@hotmail.fr, menacer_brahim@esgee-oran.dz (Corresponding author)
***University of science and the technology of Oran, L.P 1505 El-Menaour, USTO 31000Oran, Algeria*
****Department of Mechanics and advanced materials, Campus Monterrey, School of Engineering and Sciences, Tecnológico de Monterrey, Av. Eugenio Garza Sada 2501 Sur, Tecnológico, 64849 Monterrey, N.L., Mexico*
*****Mechanical Engineering Department, College of Engineering and Architecture, Umm Al-Qura University, P.O. Box 5555, Makkah 24382, Saudi Arabia*

https://doi.org/10.5755/j02.mech.35251

1. Introduction

Control of emissions in automotive systems is an important goal in current research activities, driven by the need to mitigate the harmful impacts of greenhouse gases on the environment. Achieving compliance with stringent EURO emission standards requires the adoption of specialized after-treatment technologies integrated within the engine exhaust systems to effectively reduce pollutants. Despite the anticipated transition towards electric and hybrid vehicles, there exist significant challenges, including but not limited to, the efficiency of battery charging, operational range, the time required for charging, and the sustainable generation of the electricity needed for these processes.

In response to these challenges, cutting-edge combustion technologies such as Reactivity-Controlled Compression Ignition (RCCI), Homogeneous Charge Compression Ignition (HCCI), and Premixed Charge Compression Ignition (PCCI) are being rigorously evaluated for their capacity to diminish emissions while simultaneously improving thermal efficiency. A pivotal element of this investigative effort focuses on the reduction of frictional forces, which presently represent a mere 11.5% of an engine's total energy utilization. The interaction between the piston and the cylinder liner emerges as the principal source of friction, necessitating a thorough examination of their design attributes to determine their impact on the engine's longevity and functional performance. Furthermore, the piston's lateral movements within the cylinder play a significant role in the overall frictional dynamics experienced (Fig. 1).

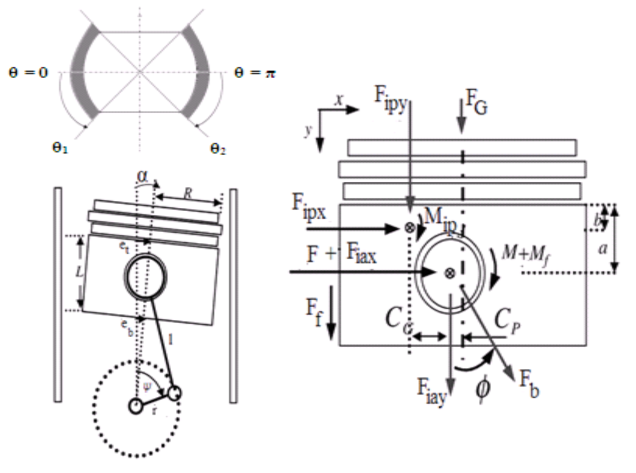

a b

Fig. 1 Piston-cylinder liner assembly a – piston lubrication system, b – piston acting forces and moments [1]

Employing the GT-SUITE software, this study aims to forecast tribological performance and quantify frictional losses within the engine. This comprehensive analysis delves into the ramifications of piston eccentricity, tilting actions, the peak oil pressure achievable, the quantification of friction power losses, the variability in oil film thickness, and the dynamics of frictional forces in relation to various crank angles, engine speeds, and operational loads. Through this meticulous examination, the study seeks to provide valuable insights into optimizing engine design and operational parameters to achieve a balance between reduced emissions and enhanced performance efficiency.

2. Literature review

Theotokatos et al. [2] used GT-SUITE based engine model capable of predicting steady-state behavior and transient response of the engine. The study utilizes a GT-ISE™ software-developed integrated engine model to assess the safety implications of marine Dual Fuel (DF) engines, focusing on steady-state behavior and transient responses. Validation against published data and subsequent simulations of fuel transitions underscored the importance of engine-turbocharger matching and wastegate control in maintaining compressor surge-free operation during fuel mode changes. Mehmet Kunt [3] studied the energy losses of a 4-stroke gasoline engine working in urban and extra-urban conditions. GT-Suite is utilized for vehicle simulation programs to assess engine and powertrain energy losses of a 4-stroke gasoline passenger car across various driving cycles, including FTP75, HFET, US06, and WLTP, both in urban and extra-urban conditions. The findings indicate that the HFET driving cycle resulted in the lowest CO2 emissions (127.58 g/km) and average fuel consumption (5.29 l/100km), with notably the lowest torque converter losses observed during this cycle (0.2%). Utilizing insights from Mehmet Kunt concentrated on enhancing the viscosity index [3]. Moreover, numerical simulations and GT-Power software validation were employed to analyze the performance of a turbocharged diesel engine, focusing on metrics like mean effective pressure, power, torque, and fuel consumption, thereby demonstrating the utility of simulation tools in enhancing engine design [4]. The cylinder deactivation (CDA) on a 16-cylinder diesel engine was studied by Liu [5]. It is shown that CDA significantly improves power and emission performances, as revealed through a comprehensive study using 1D and 3D models validated against experimental data. Findings show CDA reduces fuel consumption by up to 14% and cuts BSCO and BSsoot emissions by 75.26% and 62.9%, respectively, while slightly increasing BSFC by 0.8% without elevating BSCO emissions, showcasing its efficacy in enhancing engine efficiency and environmental compliance. Turnbull studied multi-physics analysis of piston top compression rings. The study reveals that in high-performance internal combustion engines, gas leakage losses through piston top compression rings can significantly exceed frictional losses, a novel finding not previously documented [6]. Delprete [7] summarized the synthesis of the main technical aspects and challenges regarding piston dynamics. Investigations into piston dynamics and lubrication underscore their critical role in enhancing the efficiency of internal combustion engines, significantly impacting mechanical friction, power loss, and emission reduction. Hama Rashid conducted research in a 1-D gas exchange simulation program. An engine model for natural gas buses and Miller Cycle efficiency was explored through GT-Power simulations, with a VOLVO-origin engine model, verified by varied testing cases [8]. Chris performed a powertrain Systems Analysis Toolkit (PSAT). The aim was to develop a validated simulation model of a Ford Escape Hybrid Electric Vehicle (HEV), demonstrating the model's fidelity by comparing simulated results with actual vehicle data from chassis dynamometer testing at Argonne National Laboratory. The study highlighted the potential for control strategy enhancements to boost HEV efficiency, with the model showing improvements over previous simulations [9]. Pasupathi developed a system-level battery electric vehicle model for light heavy-duty applications [10]. Mohiuddin demonstrated the effectiveness of Multi-Objective Genetic Algorithm Optimization [11]. Cerdoun et al. [12] conducted a study comparing heat transfer coefficients and temperature distributions across exhaust and intake valves at different engine speeds. The study revealed that intake valves took twice as long as exhaust valves to stabilize. This approach enables quantification of temperature distribution, thermal gradients, and thermal flux across valve zones at different engine speeds, aiding metallurgists in extending valve lifetimes. Yilmaz et al. [13] enhanced their study by incorporating the pressure ratio between the intake manifold and atmospheric pressure, along with the Reynolds number, to better understand the impact of backflow gas on intake air temperature. When compared with experimental data, they found maximum and average errors in estimating intake air temperature inside the manifold to be 2.9% and 0.9%, respectively. Nichani employed a coupled 1D-3D simulation method to accurately depict the oil sloshing phenomenon. The simulation approach efficiently models engine oil pan sloshing, significantly speeding up computational analysis while maintaining accuracy in assessing lubrication pump performance during vehicle acceleration [14]. Additionally, several hybrid versions of a traditional internal combustion engine (ICE) vehicle were compared [15]. The Miller cycle was investigated using a one-dimensional (1D) simulation model created with GT-Power software [16]. Lee used AMESim and KULI as tools in his work, a single-cylinder four-stroke diesel engine was modelled [17]. Yahuza created an engine cycle simulation for a BED (biodiesel-ethanol-diesel) fueled engine [18]. GT-Power software was utilized to predict knock and combustion [19]. Shah employed an integrated approach to conduct a 3D thermal analysis of battery cells and cooling plates [20], an innovative method was developed to analyze heat rejection calculations. A one-dimensional model of a roots-type twin rotor was studied on GT-Suite [21]. Saxena developed a real-world drive cycle [22]. Tiwari developed a simulation of tank draining using GT-SUITE [23]. A 1-dimensional CFD modeling methodology was developed using GT-SUITE [24]. In this study a one-dimensional numerical simulation model using the GT-Suite simulation software will be developed. Then numerical simulation is carried out and validated against experimental data.

3. Background

The interplay of forces and moments on an engine piston is integral to the operational dynamics and efficiency of internal combustion engines. These phenomena stem from several key sources: the combustion process, the piston's secondary movements, and the effects of inertia. The combustion force, a direct outcome of fuel-air mixture ignition within the combustion chamber, propels the piston downward during the power stroke, transforming chemical energy into mechanical work. Concurrently, the piston's vertical oscillation within the cylinder generates inertia forces, dependent on the piston's mass and its velocity's rate of change. This action results in a cyclical pattern of acceleration and deceleration, correlating with the engine's stroke phases.

Additionally, the angular trajectory of the connecting rod introduces lateral forces on the piston, compelling it towards the cylinder walls, which may lead to secondary motions such as piston slap or rock, thus impacting the engine's wear and operational efficiency. Furthermore, the synthesis of dynamic forces and the mechanical architecture of the engine-characterized by the dimensions and relationships between the piston, connecting rod, and crankshaft-give rise to moments and torsional vibrations. These forces not only affect the mechanical stress distribution across the engine's components but also have implications for the engine's longevity and smooth functionality.

A comprehensive understanding of these forces and moments is crucial for advancing engine design, mitigating component wear, and elevating the engine's performance and efficiency. This knowledge underpins the engineering strategies employed to refine the functionality of internal combustion engines, addressing both the immediate mechanical interactions within the engine and the broader implications for automotive engineering and environmental impact. The free-body diagram (FBD) in Fig. 1 is used to derive the piston motion equation. As can be seen from the FBD movement of the piston is governed by the solution of a set of equations that consider various factors acting on the piston, such as the inertia of the piston, the hydrodynamic force, the friction force, and the hydrodynamic moment. The derivation of the Forces acting in axial (y) direction, Forces acting in radial (x) direction and moments are shown in detail in Ali et.al, [25]. The general equation that governs the motion of the piston is as follows:

$$\begin{bmatrix} m_p\left(1-\frac{b}{L}\right)+m_a\left(1-\frac{a}{L}\right) & m_p\frac{b}{L}+m_a\frac{a}{L} \\ \frac{I_p}{L}+m_p\left(a-b\right)\left(1-\frac{b}{L}\right) & m_p\left(a-b\right)\frac{b}{L}-\frac{I_p}{L} \end{bmatrix}\begin{bmatrix} \ddot{e}_h \\ \ddot{e}_b \end{bmatrix}=\begin{bmatrix} F_s+F+F_f\,tan\,\phi \\ M_s+M+M_f\,l \end{bmatrix}, \tag{1}$$

with:

$$F_s=\left(F_G+F_{Ia\_y}+F_{IP\_y}\right)tan\,\phi\,, \tag{2}$$

$$M_s=F_gC_P-F_{IP\_x}C_g\,. \tag{3}$$

In this paper, we consider the thin, incompressible, and laminar oil film. The hydrodynamic pressure is calculated by solving the Reynolds equation [26]:

$$\frac{\partial}{\partial x}\left(\frac{h^3}{\mu}\frac{\partial p_h}{\partial x}\right)+\frac{\partial}{\partial y}\left(\frac{h^3}{\mu}\frac{\partial p_h}{\partial y}\right)=6U\frac{\partial h}{\partial y}+12\frac{\partial h}{\partial t}\,. \tag{4}$$

The forces and moments (F_h and M_h) are generated by the hydrodynamic pressure generated in the oil film for the surface parts limited between $\left(-\theta_1,\,\theta_1\right)$ and $\left(\theta_2,\,2\pi-\theta_2\right)$. The pressure condition for non-lubricated areas is described as:

$$p_h\left(y,\theta^*\right)=0, \qquad \theta_1\prec\theta^*\prec\theta_2\,. \tag{5}$$

The pressure reaches maximum on the edges at $\theta = 0$ and $\theta = \pi$, and is characterized by a zero-pressure gradient.

$$\left.\frac{\partial p_h}{\partial\theta}\right|_{\theta=0}=\left.\frac{\partial p_h}{\partial\theta}\right|_{\theta=\pi}\,. \tag{6}$$

The symmetry of the pressure in the oil film is expressed using the following condition:

$$p_h\left(y,-\theta\right)=p_h\left(y,\theta\right) \tag{7}$$

A pressure that at the top and at the bottom of the piston-skirt is considered to be zero:

$$p_h\left(0,\theta\right)=p_h\left(L,\theta\right)=0\,. \tag{8}$$

The hydrodynamic force and moment can be calculated by integrating the hydrodynamic pressure of the oil P_h over the lubricated area [27], [28]:

$$F_h=2R\int_0^{\pi}\int_0^{L}P_h\cos\theta\,d\theta\,dy\,, \tag{9}$$

$$M_h=2R\int_0^{\pi}\int_0^{L}P_h\left(a-y\right)\cos\theta\,d\theta\,dy\,. \tag{10}$$

Then the hydrodynamic friction force and moment around the wrist pin based on the shear stress are calculated as follows:

$$F_{fh}=2R\int_0^{\pi}\int_0^{L}\tau\,d\theta\,dy\,, \tag{11}$$

$$M_{fh}=2R\int_0^{\pi}\int_0^{L}\tau\left(R\cos\theta-C_P\right)d\theta\,dy\,. \tag{12}$$

The approximate method proposed by Zhu [29], [30] is used to calculate the contact pressure of an Aluminium piston:

$$P_c=5.464\times10^{13}\,\delta^{1.0552}\,, \tag{13}$$

where the wall deformation is denoted as δ.

Once P_c is calculated then total contact force acting on the piston skirt and moment around the wrist pin are found by:

$$F_c=2R\int_0^{\pi}\int_0^{L}P_c\cos\theta\,d\theta\,dy\,, \tag{14}$$

$$M_c=2R\int_0^{\pi}\int_0^{L}P_c\left(a-y\right)\cos\theta\,d\theta\,dy\,. \tag{15}$$

Eqs. (16) and (17) describe the contact friction force and moment of asperities in a potential solid-solid contact between the piston skirt and the cylinder.

$$F_{fc}=-2c_f R\frac{|U|}{U}\int_0^{\pi}\int_0^{L}P_c\,d\theta\,dy\,, \tag{16}$$

$$M_{fc}=2c_f R\frac{|U|}{U}\int_0^{\pi}\int_0^{L}P_c\left(R\cos\theta-C_P\right)d\theta\,dy\,. \qquad 17)$$

where c_f is empirical friction coefficient of the solid.

Considering that the oil film is fixed to the piston during its movement, its thickness is closely related to the secondary motion of the piston. Neglecting elastic deformation, the thickness of the lubricating film can be calculated using the following expression:

$$h\left(\theta,y,t\right)=c+e_t\left(t\right)\cos\varphi+ \\ +\left[e_b\left(t\right)-e_t\left(t\right)\right]\frac{y}{L}\cos\varphi\,. \tag{18}$$

The lubricant's dynamic viscosity is given by [16]:

$$\mu=\frac{5.6625\times10^4}{\left(T+40\right)^{4.5067}}\rho\,. \tag{19}$$

Shear force and hydrodynamic friction are given as [26]:

$$\tau = -\frac{U\mu}{h}\left(\Phi_f + \Phi_{fs}\right) + \frac{h}{2}\frac{\partial P}{\partial x}\Phi_{fp}, \tag{20}$$

where Φ_f, Φ_{fs}, Φ_{fp} are the shear pressure factors.
The power loss is given by:

$$P_u = F \times U = U \times \int_0^L \tau(x)dx. \tag{21}$$

3. Results and discussions

Table 1 presents the diesel engine specifications data used in GT-SUITE simulation. The influence of engine speed and engine load on the tribological behavior of the piston-cylinder contact is studied due to their significant importance.

Table 1

Engine specifications

Parameters	Values	Units
Bore	119	mm
Stroke	87.5	mm
Connecting road	300	mm
Compression ratio	17:1	-
Cylinders number	01	-
Timing of injection	10°	BTDC
Opening of intake valve	11°	BTDC
Clouse of intake valve	32°	ABDC
Opening of exhaust valve	35°	BBDC
Closure of exhaust valve	16°	ATDC
Oil type	SAE 30	-

Simulation results are verified against experimental data from the work of Lee et al. [17]. Fig. 2 shows the variation of the hydrodynamic friction force between the compression ring and the cylinder as a function of the rotation angle for an engine speed of 2000 rpm and partial load. The same engine parameters were introduced into the simulation software to calculate this friction force. The simulation results are in agreement with the work of Lee et al. [17], with a satisfactory match between the simulated and experimental data. The maximum friction force occurs at the point of maximum pressure in the cylinder. The negative part of the curve is due to the change in direction of the piston velocity resulting from the reciprocating motion.

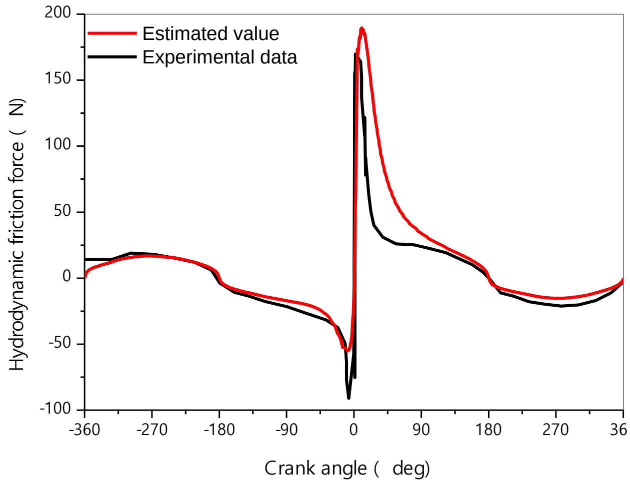

Fig. 2 Top ring hydrodynamic friction force versus crank angle

3.1. Engine speed effect

Fig. 3 illustrates the impact of the engine speed on the piston eccentricity at full load for one engine cycle. It can be observed that the maximum eccentricity values decrease as the engine rotation speed increases during the combustion, expansion, and exhaust phases. On the other hand, during the intake and compression phases, these maximum values increase with the motor rotation speed.

Fig. 4 shows the effect of the engine speed on the piston tilt angle at full load for one engine cycle. A significant influence is observed during the expansion period. The maximum tilt angle values decrease as the motor rotation speed increases.

Fig. 5 presents the effect of the motor speed on the minimum oil film thickness on the main thrust side between the piston and the cylinder liner at full load. In general, the oil film thickness increases with the increase of motor speed during the intake and compression strokes, and decreases during the expansion and exhaust strokes. It can be observed that the minimum oil film thickness is reached during the expansion stroke.

Fig. 6 illustrates the impact of engine speed on the maximum oil film pressure in the major thrust of the piston-cylinder assembly at full load for one engine cycle. The oil pressure reaches its maximum value in the middle of each

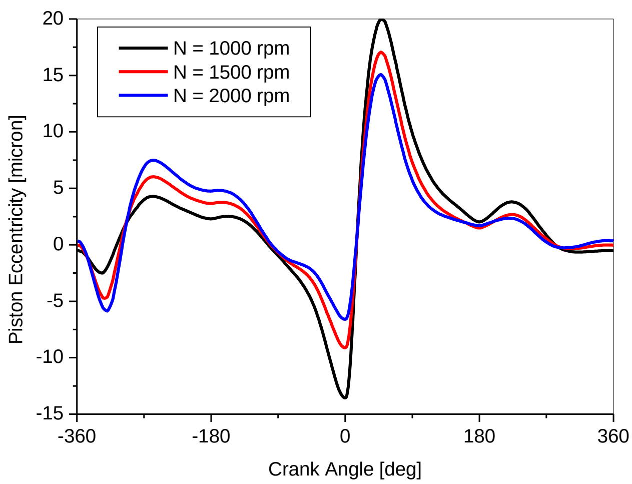

Fig. 3 Engine speed effect on piston eccentricity versus crank angle

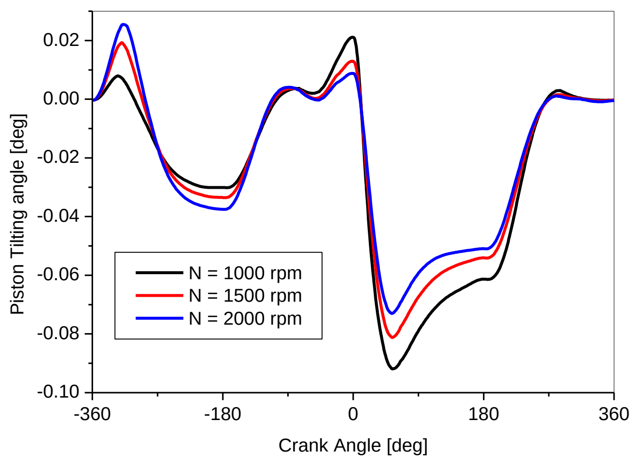

Fig. 4 Engine speed effect on piston tilting versus crank angle

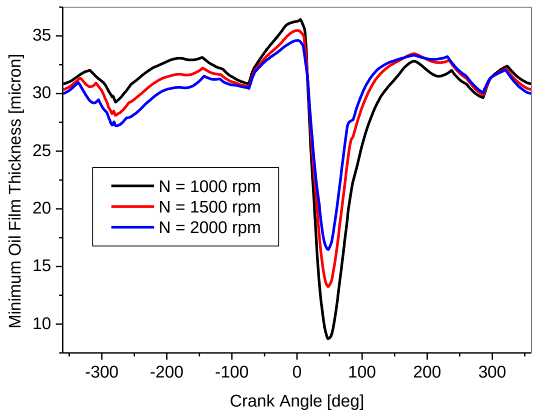

Fig. 5 Engine speed effect on minimum oil film thickness versus crank angle

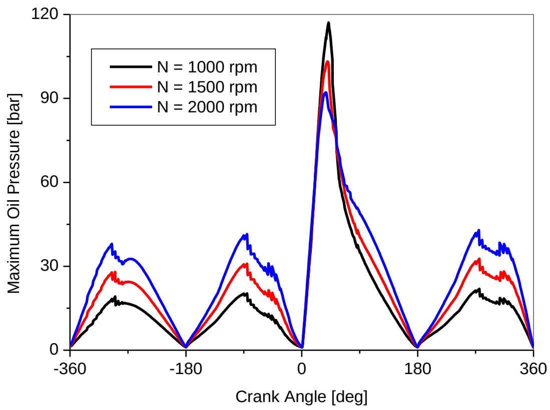

Fig. 6 Engine speed effect on maximum oil pressure versus crank angle

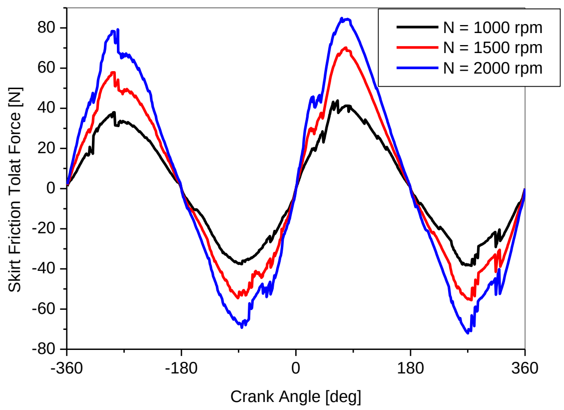

Fig. 7 Engine speed effect on skirt friction total force versus crank angle

stroke for all three engine speeds. During the intake, compression, and exhaust strokes, the maximum oil pressure increases with engine speed and can reach a value of 30 bars. On the other hand, the maximum oil pressure decreases with increasing engine speed during the expansion stroke, with a peak of 118 bars possible at a speed of 1000 rpm.

Fig. 7 presents the effect of the engine speed on the total hydrodynamic friction force of the oil film in the piston skirt-cylinder liner assembly at full load for one engine cycle. For the three engine rotation speeds, it can be observed that the friction force reaches its maximum value in the middle of each stroke, and zero values when the piston is at TDC (top dead center) and BDC (bottom dead center). The

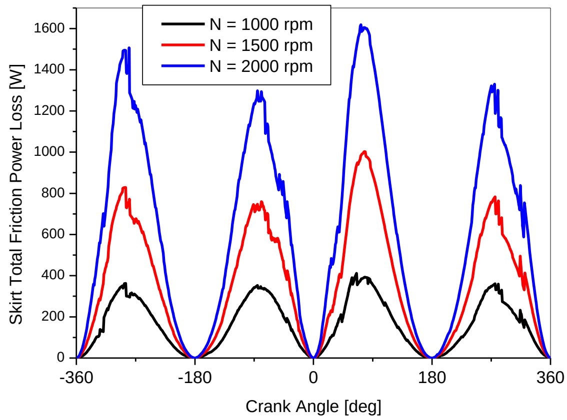

Fig. 8 Engine speed effect on skirt total friction power loss versus crank angle

maximum value of the hydrodynamic friction force is 80 N for an engine speed of 2000 rpm.

Fig. 8 shows the effect of the engine speed on the total hydrodynamic friction power of the oil film in the piston skirt-cylinder liner assembly at full load for one engine cycle. There is a remarkable influence of the engine rotational speed. The friction power reaches its maximum value in the middle of each stroke and zero values when the piston is at TDC and BDC. The hydrodynamic friction power can reach a maximum value of 1.5 kW.

3.2. Engine load effect

The engine load effect on the piston eccentricity during one cycle of the engine operating at 1000 rpm is demonstrated in the Fig. 9. The graph clearly shows that as the engine load increases, the maximum eccentricity values also increase during both the combustion and expansion phases. In fact, if the engine load were to increase by 25%, the maximum value of piston eccentricity would increase by 35%.

The impact of the engine load on the piston tilt angle during one cycle of the engine running at 1000 rpm is presented in Fig. 10. The graph highlights that there is a significant influence on the piston tilt angle during the combustion and expansion period, where the maximum tilt angle values decrease as the engine load increases.

Fig. 11 illustrates the evolution of the minimum oil film thickness between the piston and cylinder liner on the main thrust side versus crank angle for different engine load during one engine cycle and engine speed of 1000 rpm. The graph reveals that, overall, the oil film thickness decreases as the engine load increases across all engine strokes. Additionally, the minimum value for the oil film thickness is observed during the expansion stroke.

The impact of the engine load on the maximum oil film pressure in the major thrust of the piston-cylinder assembly during one cycle of the engine operating at 1000 rpm is presented in Fig. 12. The graph indicates that the oil pressure reaches its highest value in the middle of each stroke, regardless of the engine load. However, the maximum oil pressure varies significantly during the expansion stroke, where it increases with the engine load and can reach a peak of 98 bars at full load.

Fig. 13 illustrates the relationship between engine load and the total hydrodynamic friction force of the oil film

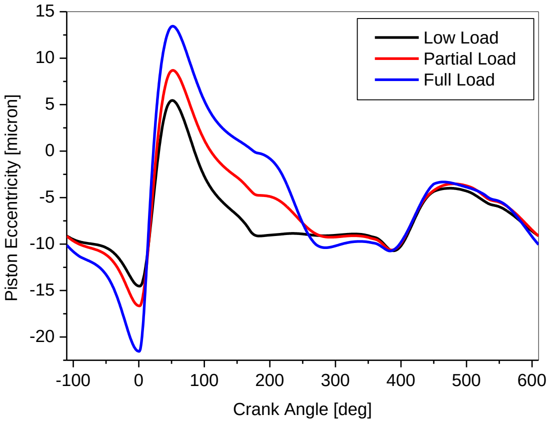

Fig. 9 Engine load effect on piston eccentricity versus crank angle

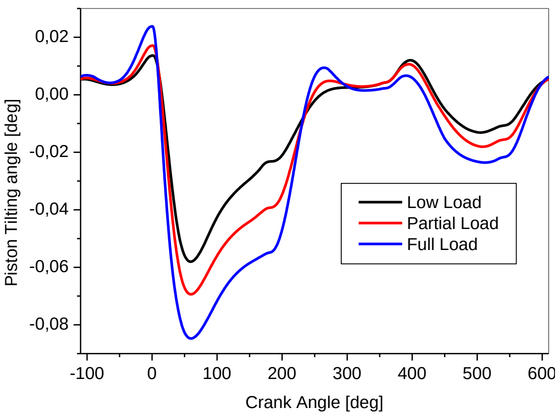

Fig. 10 Engine load effect on piston tilting versus crank angle

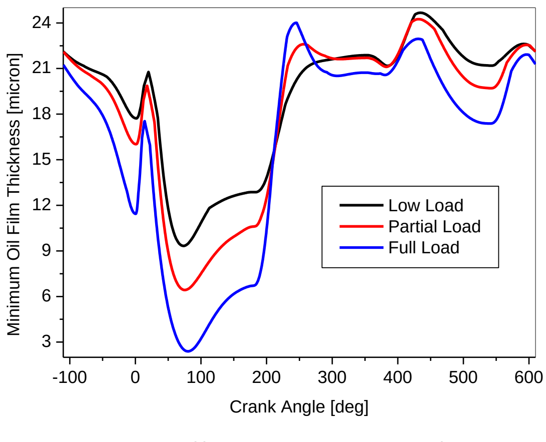

Fig. 11 Engine load effect on minimum oil film thickness versus crank angle

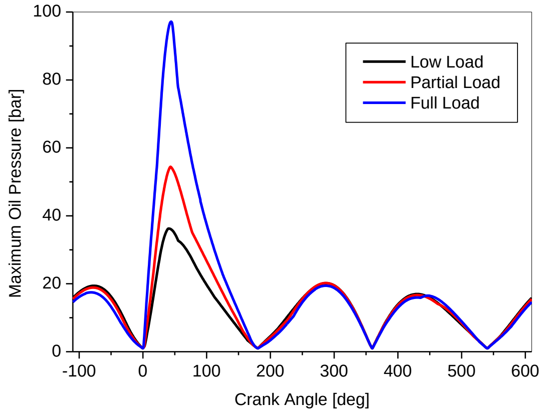

Fig. 12 Engine load effect on maximum oil pressure versus crank angle

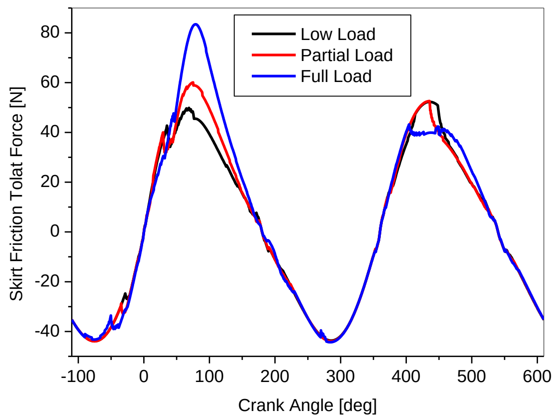

Fig. 13 Engine load effect on skirt friction total force versus crank angle

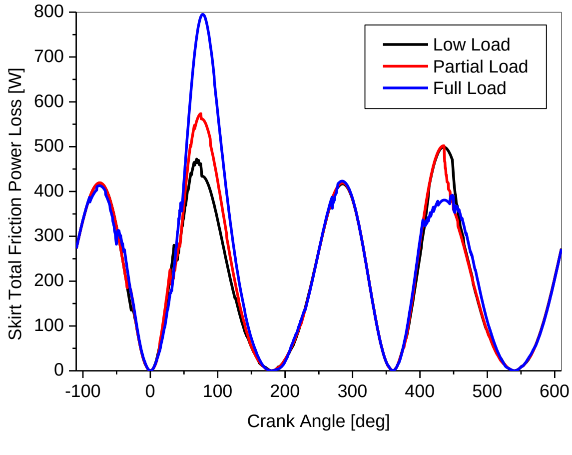

Fig. 14 Engine load effect on skirt total friction power loss versus crank angle

in the piston skirt-cylinder liner assembly. The data pertains to an engine speed of 1000 rpm and a single engine cycle. It can be observed that regardless of the engine load, the friction force reaches its peak during the midpoint of each stroke, with zero values occurring when the piston is at TDC (top dead center) and BDC (bottom dead center). According to the data, the maximum hydrodynamic friction force is 80 N when operating at full load.

The effect of the engine load on the total hydrodynamic friction power of the oil film in the piston skirt-cylinder liner assembly during one cycle of the engine operating at 1000 rpm is depicted in Fig. 14. The graph indicates that the friction power reaches its highest value in the middle of each stroke and has zero values when the piston is at TDC (top dead center) and BDC (bottom dead center). Additionally, there is a notable influence of the engine load during the expansion period, where the friction power can reach a maximum value of 0.8 kW at full load.

4. Conclusions

In this research, we have successfully formulated and validated a one-dimensional numerical simulation model utilizing the GT-Suite simulation platform, achieving a noteworthy correlation between the simulated outcomes and empirical data. This model's validation underscores its efficacy in accurately replicating the dynamic behavior of internal combustion engines under varied operational conditions.

Our findings illuminate the critical influence of engine speed and load on the tribological interactions within the piston-cylinder interface, highlighting their pivotal role in modulating frictional losses. Specifically, adjustments to these parameters emerged as effective strategies for enhancing tribological efficiency, thereby heralding potential advancements in engine design for optimized performance. Notably, the study revealed a reduction in oil film thickness during the piston's expansion phase, attributed to elevated oil pressures, which underscores the intricate relationship between engine operational parameters and lubrication dynamics.

Despite the comprehensive nature of this study, it recognizes the existence of additional complex phenomena not yet explored, which could substantially affect the engine's tribological performance. Future research endeavors will aim to integrate the effects of piston bore distortion, focusing on its implications for the piston-cylinder assembly's sealing efficiency and mass flow dynamics. This expanded analytical framework is anticipated to yield deeper insights into the nuanced mechanisms governing engine performance, paving the way for the development of more refined and efficient internal combustion engines.

References

1. **Belahcene, M.; Mazouzi, R.** 2018. Numerical Study of Thermal Effect on the Friction of Piston-cylinder Contact in an Internal Combustion Engine, Tribology in Industry 40(4): 643-653. https://doi.org/10.24874/ti.2018.40.04.11.
2. **Theotokatos, G.; Stoumpos, S.; Bolbot, V.; Boulougouris, E.** 2020. Simulation-based investigation of a marine dual-fuel engine, Journal of Marine Engineering & Technology 19(sup1): 5-16. https://doi.org/10.1080/20464177.2020.1717266.
3. **Mehmet, A. K.** 2022. Analysis of Engine and Powertrain Losses of a Passenger Type 4-Stroke Gasoline Vehicle in 4 Different Driving Cycles with GT-Suite Vehicle Simulation Program, International Journal of Automotive Science and Technology 6(4): 340-346. https://doi.org/10.30939/ijastech..1152980.
4. **Vdovin, A.** 2010. Cooling performance simulations in GT-Suite, Master's Thesis in the Master's programme Automotive Engineering. ISSN 1652-8557.
5. **Liu, Y.; Kuznetsov, A.; Sa, B.** 2021. Simulation and Analysis of the Impact of Cylinder Deactivation on Fuel Saving and Emissions of a Medium-Speed High-Power Diesel Engine, Applied Sciences 11: 7603. https://doi.org/10.3390/app11167603.
6. **Asfoor, M. S.; Sharaf, A. M. and Beyerlein, S.** 2014. Use of GT-suite to study performance differences between internal combustion engine and hybrid electric vehicle powertrains, 16th International Conference on Applied Mechanics and Mechanical Engineering: 1-16. https://doi.org/10.21608/amme.2014.35473.
7. **Delprete, C.; Razavykia, A.** 2018. Piston dynamics, lubrication and tribological performance evaluation: A review, International Journal of Engine Research 21(5): 725-741. https://doi.org/10.1177/1468087418787610.
8. **Menacer, B.; Mostefa, B.** 2013. Numerical simulation and prediction of the performance of a direct injection turbocharged diesel engine, SIMULATION: Transactions of The Society for Modeling and Simulation International 89(11): 1355-1368. https://doi.org/10.1177/0037549713499249.
9. **Mi, C.; Masrur, M.A.** 2017. Modeling and Simulation of Electric and Hybrid Vehicles. In Hybrid Electric Vehicles (eds C. Mi and M.A. Masrur): 409–431. https://doi.org/10.1002/9781118970553.ch14.
10. **Pasupathi, S.; Shetty, A.; Rathod, S.; Bergsieker, G.** 2019. System Level Vehicle Model Development of Light Heavy Duty Battery Electric Vehicle in GT-Suite, SAE Technical Paper: 2369, https://doi.org/10.4271/2019-01-2369.
11. **Mohiuddin, A. K. M.; Rahman, M. A.; Shin, Y. H.** 2011. Application of Multi-Objective Genetic Algorithm (MOGA) for Design Optimization of Valve Timing at Various Engine Speeds, Advanced Materials Research 264-265: 1719–1724. https://doi.org/10.4028/www.scientific.net/amr.264-265.1719.
12. **Cerdoun, M.; Khalfalah, S.; Beniaiche, A.; Carcasci, C.** 2019. Investigations on the heat transfer within intake and exhaust valves at various engine speeds, International Journal of Heat and Mass Transfer 147: 119005. https://doi.org/10.1016/j.ijheatmasstransfer.2019.119005.
13. **Yilmaz, E.; Ichiyanagi, M.; Suzuki, T.** 2019. Development of Heat Transfer Model at Intake System of IC Engine with Consideration of Backflow Gas Effect, International Journal of Automotive Technology 20: 1065-1071. https://doi.org/10.1007/s12239-019-0100-1.
14. **Nichani, V.; Zhou, Z.; Gao, H.; Gendron, S.** 2020. A Direct 1D/3D (GT-SUITE/SimericsMP+) Coupled Computational Approach to Study the Impact of Engine Oil Pan Sloshing on Lubrication Pump Performance, SAE Technical Paper 2020-01-1112. https://doi.org/10.4271/2020-01-1112.
15. **Graziano, E.; Bruno, L.; Corrado, P.; Pierson, S.** 2019. Set-Up and Validation of an Integrated Engine Thermal Model in GT-SUITE for Heat Rejection Prediction, SAE Technical Paper 2019-24-0078. https://doi.org/10.4271/2019-24-0078.
16. **Hamarashid, L.** 2018. GT-Power Modeling of a 6-Cylinder Natural Gas Engine and Investigation of the Possible Performance Improvements by Studying the Miller Cycle, Lund university Master's thesis. Available at: http://lup.lub.lu.se/student-papers/record/1429536.
17. **Lee, S.; Kang, J.; Park, S.** 2020. Measurement and modeling of crank train friction in light - duty diesel engines, Journal of Mechanical Science and Technology 34(2): 889-903. https://doi.org/10.1007/s12206-020-0139-y.
18. **Yahuza, I.; Dandakouta, H.; Ibrahim, M. H.; Dasin, D. Y.** 2018. Modelling and Simulation of Some Combustion Parameters (Intport-1 and Intvalve-1) using Gt-Power Engine Simulation Software with Biodiesel-Ethanol-Diesel Blends as Fuel, International Journal of Trend in Scientific Research and Development 3(1): 1206-1214. http://dx.doi.org/10.31142/ijtsrd19188.

19. **Neelakandan, K.; Goutham, S. M.; Tushar, D.; Pooja N.** 2014. Numerical Prediction of Vehicle Front End Module Effects on Engine Cooling System Performance, International Journal of Engineering and Advanced Technology, 4(2): 73-78. Available at: https://www.ijeat.org/portfolio-item/b3605124214/
20. **Shah, S.; Vijay, D.; Lehocky, M.** 2020. Thermal Management of Electrified Vehicle by Means of System Simulation. SAE Technical Paper 2020-28-0033. https://doi.org/10.4271/2020-28-0033.
21. **Wei, S.; Zhang, Z.; Li, X.; Wu, C.; Yang, F.** 2022. Simulation Analysis of Fuel Economy of the GDI Engine with a Miller Cycle and EGR Based on GT-Power, Processes 10(2): 319. https://doi.org/10.3390/pr10020319.
22. **Saxena, S.; Kudachi, B.; Pasupathi, S.; Bergsieker, G.** 2023. Commercial Vehicle – Drive Cycle Development and Validation Using GT-Real Drive & 1D GT-SUITE Electric Vehicle Models. SAE Technical Paper 2023-01-0472. https://doi.org/10.4271/2023-01-0472.
23. **Tiwari, A.; Framke, N.** 2019. Modeling Fuel Tank Draining/Sloshing in a Typical Transiently Accelerating Vehicle using GT-SUITE for Reliable Tank Designing, SAE Technical Paper 2019-01-1262. https://doi.org/10.4271/2019-01-1262.
24. **Mazouzi, R.; Maspeyrot, P.; Kellaci, A.; Rahal, D. D.** 2009. Effet des paramètres de conception du piston sur le frottement jupe-chemise, Mécanique & Industries 10(2): 91-101. https://doi.org/10.1051/meca/2009037.
25. **Ali, A. M.; Xianjun, H.; Turkson, R.; Ezzat, M**. 2015. An analytical study of tribological parameters between piston ring and cylinder liner in internal combustion engines. Proceedings of the Institution of Mechanical Engineers, Part K, Journal of Multi-body Dynamics 230(4): 329-349. https://doi.org/10.1177/1464419315605922.
26. **Menacer, B.; Bouchetara, M.** 2020. Numerical study of the effect of first ring profile type on hydrodynamic performance of the lubricant in diesel engine. Revista De Metalurgia 56(3): e177. https://doi.org/10.3989/revmetalm.177.
27. **Salaheldin, A.M.; Zheng, Q.; Lu, X.Q.; Guo, Y.B.; Zhu, J.Z.** 2014. Numerical Simulation of Piston Ring Lubrication with Multi-grade Oil, Applied Mechanics and Materials 595: 83-90. https://doi.org/10.4028/www.scientific.net/AMM.595.83.
28. **Turnbull, R.; Dolatabadi, N.; Rahmani, R.; Rahnejat, H.** 2020. An assessment of gas power leakage and frictional losses from the top compression ring of internal combustion engines, Tribology International 142: 105991. https://doi.org/10.1016/j.triboint.2019.105991.
29. **Zhu, D.; Cheng, H. S.; Arai, T.; Hamai, K.** 1992. A Numerical Analysis for Piston Skirts in Mixed Lubrication—Part I: Basic Modeling, ASME Journal of Tribology 114(3): 553-562. https://doi.org/10.1115/1.2920917.
30. **Zhu, D.; Cheng, H. S.; Hu, Y. Z.; Arai, T.; Hamai, K.** 1993. A Numerical Analysis for Piston Skirts in Mixed Lubrication: Part II – Deformation Considerations, ASME Journal of Tribology 115(1): 125-133. https://doi.org/10.1115/1.2920965.

B. Menacer, A. Soualmia S. Narayan, M. Al-lehaibi

IMPACT ANALYSIS OF KEY ENGINE PARAMETERS ON PISTON LUBRICATION AND FRICTION PERFORMANCE IN DIESEL ENGINES USING GT-SUITE PROGRAM

S u m m a r y

In Compression ignition engines combustion occurs at higher temperatures that leads to a rapid rise in combustion pressure and amount of heat released. This may lead to lesser emissions during engine cycle. Moreover, occurrence of combustion takes place for a very small crank angles duration resulting in better thermal efficiency. On the other hand, the oil used for lubrication in IC engines is responsible for a significant amount of pollution and particles emitted into the environment. In order to comply with increasingly strict pollution standards, manufacturers make considerable efforts to minimize the impact of oil consumption on engine emissions. The purpose of this study is to develop a one-dimensional numerical simulation method using GT-Suite software to assess how the engine speed and load affect the oil film thickness, frictional force, and power losses during the operating engine cycle. The results obtained in this simulation were validated using experimental data, and there is good agreement between the numerical and experimental results. It was found in this paper that the maximum friction power losses were found to be 1.6 kW at middle of strokes and the minimum Oil film thickness was obtained in range of 9-38 μm.

Keywords: Engine friction, piston, cylinder liner, internal combustion engine, GT- SUITE software, lubrication.

Received October 3, 2023
Accepted June 20, 2024